Astron. Astrophys. 333, 803–808 (1998)

ASTRONOMY AND ASTROPHYSICS

Dust properties of NGC 2076 ⋆

D.K. Sahu[1], **S.K. Pandey**[1,2], **and Ajit Kembhavi**[3]

[1] School of Studies in Physics, Pt. Ravishankar Shukla University, Raipur, 492 010, India
[2] School Of Physical Sciences, SRTM University, Nanded, 431 602, India
[3] IUCAA, Post Bag 4, Ganeshkhind, Pune, 411 007, India

Received 10 September 1997 / Accepted 27 January 1998

Abstract. We present multiband CCD surface photometry of NGC 2076, an early-type galaxy with a broad dust lane. We investigate the wavelength dependence of the dust extinction and derive the apparent extinction law. The extinction varies linearly with inverse wavelength with a ratio of total to selective extinction R_V = 2.70±0.28. The smaller value of R_V relative to the Galactic value implies that the size of 'large' dust grains, responsible for extinction, is smaller than that in our Galaxy. We calculate the dust mass from total extinction, as well as from the color excess. We use IRAS data on FIR emission to determine the dust temperature, star formation rate and star formation efficiency.

Key words: galaxies: individual: NGC 2076 – dust, extinction – galaxies: elliptical and lenticular, cD – galaxies: ISM – galaxies: photometry

1. Introduction

Dust is now known to be frequently present in early-type galaxies, detected through optical (Hawarden et al. 1981, Ebneter & Balick 1985, Ebneter et al. 1988) as well as FIR emissions (Jura et al. 1987, Knapp et al. 1989). These studies have reported the dust detection rate in E's as 36% and in SO's as 50%, suggesting that dust is more frequent in SO's than in E's. The study of Goudfrooij et al. (1994a) revealed an optical detection rate of dust in E's as 41%. However, taking into consideration the misclassification of E's and SO's (selection effects) could very well raise the estimate to a value as high as 80% in case of E's. The HST survey of these galaxies has shown presence of dust in the nuclei of almost every galaxy (Jaffe et al. 1994).

The other phases of the interstellar matter (ISM) i.e. hot, warm and cool gas are also observed in these galaxies. Hot gas ($\sim 10^7$K) is observed through X-ray emission (Forman et al. 1985, Fabbiano et al. 1992) of coronal gases having typical mass of the order of $\sim 10^9$ - $10^{10} M_\odot$, which is consistent with the expected amount from the accumulated stellar mass loss, heated by collision and gravity (Fabian et al. 1987, Sarazin 1986 and references therein). Warm gas ($\sim 10^4$K) observed through line emission contributes only 10^3 - $10^5 M_\odot$ to the total ISM content in these galaxies (Phillips et al. 1986, Caldwell 1984). Around 55% of these galaxies are known to contain this less dominant but physically interesting component (Sadler 1984, Kim 1989, Goudfrooij et al. 1994a). Substantial amount of cool gas ($< 10^2$K) is also detected in these galaxies, through HI mapping and far infrared emission from them (Knapp et al. 1985, 1989). These galaxies are also found to contain the molecular clouds, as evident from CO emission detected in many of them (Lees et al. 1991, Wang et al. 1992, Wiklind et al. 1995).

Dusty ellipticals have received systematic attention after Bertola and Galleta (1978) realized their importance in determining three dimensional structure of these galaxies (van Albada et al. 1982), and in studying the origin and subsequent evolution of the interstellar matter and the underlying galaxy (Faber and Gallagher 1976, Schweizer 1987). Further, the broad dust lane in these galaxies were also used to investigate properties of dust in extragalactic environments (Rodgers 1978, Brosch et al. 1985, 1990, 1991, Goudfrooij et al. 1994b).

Orientation of dust lanes can be used as an additional information to infer the intrinsic shapes of ellipticals. The cold gas and dust is expected to be in simple closed orbits in the galaxy potential, which occur in a small number of preferred planes (Gunn 1979, Habe & Ikeuchi 1985, 1988). Thus the kinematics and morphology of these disks/lanes can be used to constrain intrinsic shapes of the underlying galaxy.

Early-type galaxies are suitable targets to study the dust grain properties in the extragalactic environments. The data can be used to model the size distribution of grains (Rowan-Robinson 1992), to predict the different mechanisms operating (de Jong et al. 1990, Drain & Saltpeter 1979, Barlow 1978), to make the existence of dust possible in a wide variety of environments. As pointed out by Goudfrooij et al. (1994b) the physical properties of dust are a function of time and can be used as indicator for the time elapsed since the dust was last substantially replenshied. The basic tool to study the dust properties is to examine the behaviour of dust extinction in different wavebands i.e. the extinction curve. There are two main methods to determine the wavelength dependence of dust extinction in galaxies: (i) Direct method - This method is used to study the dust properties of our own Galaxy. The extinction curve is plotted with the help of stellar photometry of individual stars, whose intrin-

⋆ Based on observations taken from VBO, Kavalur, India

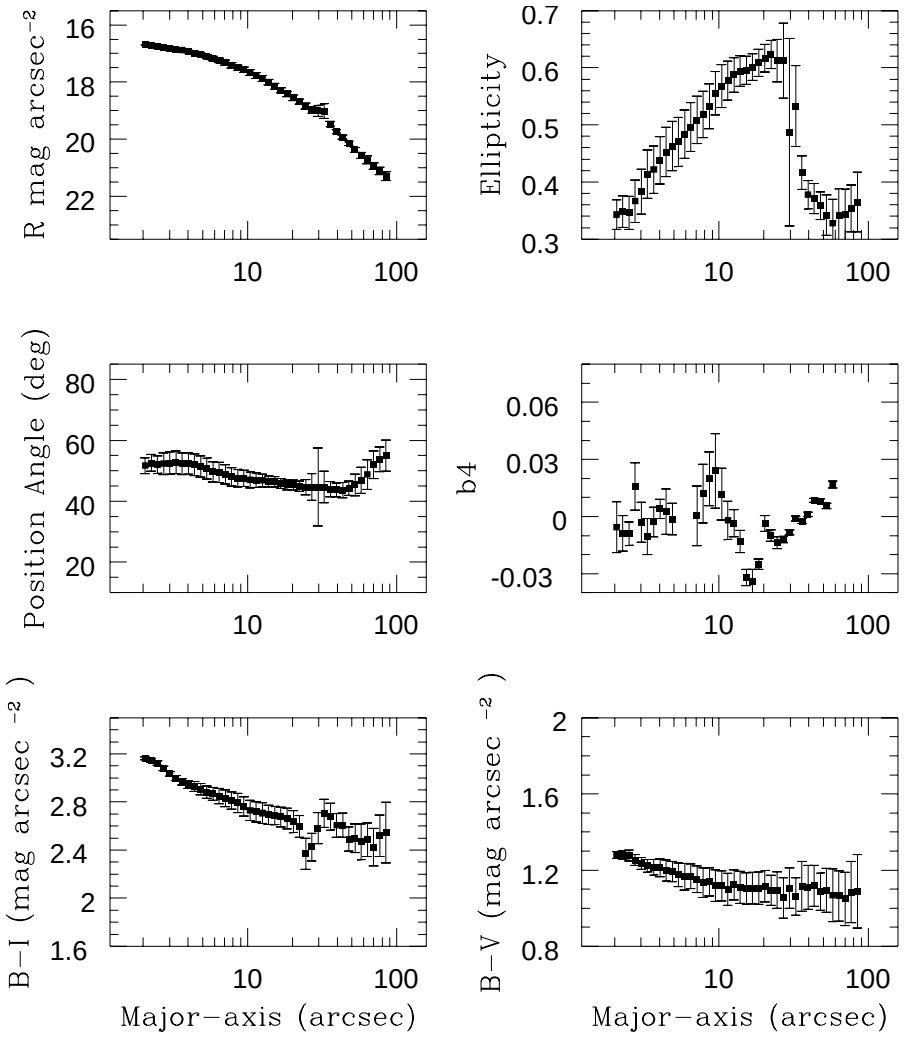

Fig. 1. The R band profiles of surface brightness, ellipticity, position-angle, amplitude of residual cos4θ co-efficient of the isophotal deviation from the best fitting ellipse (b_4), and color-index profiles.

Table 1. Observational parameters of NGC 2076

1. Alternative names: MGC -03-15-12, IRAS 05445-1648, PGC 17804.
2. Position (epoch 1950): $\alpha = 05^h44^m33^s.6$; $\delta = -16^o47^m59^s$.
3. Dimensions: 2′.2 x 1′.3.
4. Velocity: 2156 km s^{-1}.
5. Photometric properties:
(a). Magnitude: B_T=14.0.
(b). Colors: $(B-V)_T$=1.01±0.02 ; $(U-B)_T$=0.43±0.04.
6. FIR flux:
. f(12μm) = 0.77±0.029 Jy.; f(25μm)=0.90±0.037 Jy.; f(60μm) = 14.62±0.047; f(100μm)=30.10±0.12 Jy.
7. Radio Properties:
(a). Total flux density at 1.425 GHz.: 57.8 mJy.
(b). Absolute spectral luminosity at 1.425 GHz log(L): 21.81 WHz^{-1}.
(c). Integrated flux density: 57.3 mJy.

sic luminosity is known by means of some other methods. It is found that the Galactic extinction curve is a function of R_V, the ratio of total selective extinction A_V in V band to the selective extinction E_{B-V} between B and V bands.
(ii) Indirect method - In extragalactic objects photometry of individual stars is not possible and hence indirect methods for calculating R_V are used. Comparison between the original galaxy (extinguished) and a smooth model (unextinguished) gives an estimate of extinction by dust; this exercise at a number of wavelength gives the extinction law. Several workers have used these indirect methods and determined values of R_V for spiral galaxies (Knapen et al. 1991, Lequeux 1988, Walterbos & Kennicutt

1988) quite similar to that in our Galaxy. On the other hand the value of R_V for early-type galaxies is smaller than the Galactic value (Goudfrooij et al. 1994b).

In this paper we report detailed study of the dusty galaxy NGC 2076. This galaxy has been classified as lenticular in the Third Reference Catalogue (RC3) of Bright Galaxies (de Vaucouleurs et al. 1991). As the dust lies parallel to the major axis, Ebneter & Balick (1985) have categorised the dust configuration as oblate. Mollenhoff et al. (1992) carried out 20cm. radio observation for a sample of dusty ellipticals to examine the connection between optical morphology of radio galaxies and the orientation of the radio jets. All dust lane ellipticals with radio jets show a strong tendency for radio jets to be orthogonal to the dust lane. NGC 2076 posses a strong dust lane along its apparent major axis. The low resolution radio map shows an extended radio source of size 37″ x 20″ centered on the optical source. However, its high resolution radio maps does not reveal any radio structure. NGC 2076 is also enlisted in the 1.425 GHz atlas of IRAS Bright Galaxy Sample studied by Condon et al. (1996). Its optical, infra-red and radio properties collected from RC3 (1991), Knapp et al. (1989), and Condon et al. (1996), respectively, are given in Table 1.

2. Observation and reduction

Broad band Johnson B, V and Cousins R and I images of NGC 2076 were taken at the Prime focus of the 2.3m Vainu Bappu telescope of the Vainu Bappu Observatory, Kavalur, India during March, 1996, as a part of a CCD imaging programme on a sample of early-type galaxies. The observations were carried out using a 1024 $\times$ 1024 chip with pixel size 24 μm square pixels in direct imaging mode. This gives a scale of 0″.63 per pixel and a total field of $10'.75 \times 10'.75$. We obtained one frame each in B, V, R and I filters, with exposure times 40, 30, 15 and 15 minutes respectively, to obtain good signal-to-noise ratio in all the filters. Observations were taken under photometric conditions and seeing was in the range 2″.5 - 3″.0 (FWHM). Several sky flats in each filter and bias frames were taken for pre-processing of the CCD data.

Cleaning of these images was done using standard tasks within IRAF [1]. Galaxy frames in different filters were aligned to an accuracy better than 0.1 pixel by translation. These frames were convolved with gaussian to make seeing of the best frame comparable to the worst one. The field of view of our telescope-detector combination was large $\sim$11′x11′, so we could easily select regions far off from the galaxy and not affected by the foreground stars, to get the sky background.

[1] IRAF *is distributed by the National Optical Astronomy Observatories (NOAO), which is operated by the Association of Universities, Inc. (AURA) under co-operative agreement with the National Science Foundation.*

3. Analysis technique

The isophotal shape analysis was carried out using the 'ellipse' task within "STSDAS"[2], which is based on the method described in detail by Jedrzejewski (1987). The dust lane crosses the galaxy close to the center and hence determination of its center accurately is difficult. The I band image is least prone to the dust extinction, so we have determined the center of the median filtered I band image and used the same center for isophotal shape analysis of all the well aligned frames. While fitting ellipses to the isophotes, the center thus determined was kept fixed. We have derived the surface brightness and shape parameters of this galaxy by masking out the regions occupied by the dust lane and foreground stars. Previous work on this galaxy include a comparison of optical image with the radio map to look for the orientation of radio source with respect to the prominent dust lane on the galaxy (Mollenhoff et al. 1992), and its aperture photometry in optical broad band filters by Boisson et al. (1994). Detailed surface photometry of this galaxy has not been reported in the literature. We have used the aperture photometry of Boisson et al. (1994) to calibrate our frames. Simulated aperture photometry was performed using circular apertures to determine zero point constants for calibration. The surface brightness profile and shape parameter profiles are shown in Fig.1. The parameter b_4 characterizes the deviation of isophote from the pure ellipse and it appears as the co-efficient of the fourth order cosine term of the Fourier expansion of the ellipse fitting procedure.

3.1. Generation of color-index and extinction maps

Color-index map: To calculate the mass of the dust residing in the galaxy we have generated the color-index maps (B-V, V-R, B-I, V-I) using the broad band images. These maps were used to determine the dust distribution and color-excess in the dusty region. The B-I color map is shown in Fig. 2.

Extinction maps: The amount of extinction is determined by comparing the actual light distribution collected from the galaxy with that expected in the absence of dust lane. The extinction map was generated by dividing the original galaxy frame by a smooth model of it. The smooth model was obtained using the isophotal parameters generated by the ellipse fitting process. While fitting ellipses the regions occupied by dust and foreground stars were masked and ignored. The fits were carried out with all the fitting parameters allowed to vary, except the center. By applying polynomial fit to the fitted data a smooth model of the galaxy was obtained. The model images were used to get the extinction map at each wavelength in the following manner

$$A_\lambda = -2.5 \log(I_{\lambda,obs}/I_{\lambda,model}), \quad (1)$$

where, I stands for the ADU counts. This gives the desired extinction map in magnitude scale.

Extinction curve: The extinction maps in different filters were

[2] The Space Telescope Science Data Analysis System STSDAS is distributed by the Space Telescope Science Institute.

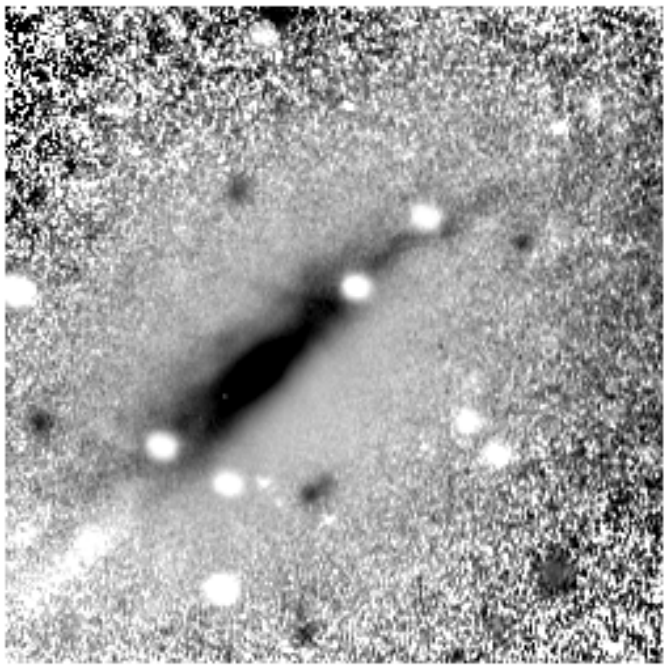

Fig. 2. B-I color index image of the galaxy NGC 2076; darker shades represent redder regions. East is up and north is to the right.

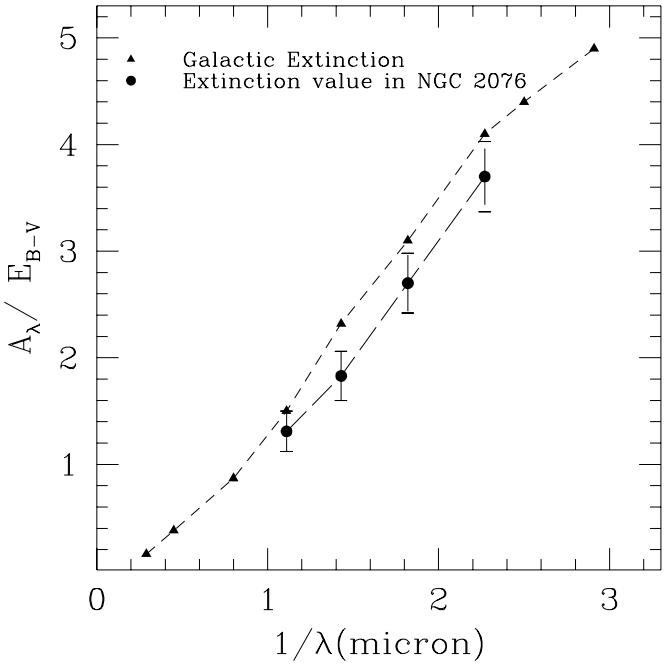

Fig. 3. Extinction curve for NGC 2076 alongwith the Galactic extinction curve.

used to determine the extinction due to the dust lane. We chose a rectangular box of size three times the seeing disk, and slided it over the whole region covered by dust to determine the numerical values of local extinction A_λ(λ = B, V, R, I). The local color-excess or selective extinction were also calculated using the relation

$$E(\lambda - V) = A_\lambda - A_V \quad (2)$$

For determining the ratio of total to selective extinction we have used the method discussed by Brosch et al. (1990) and Goudfrooij et al. (1994b). Linear regression between the different extinction values were calculated and the best fitting slopes were assigned to be the average of the slope of A_X Vs. A_Y and the reciprocal slope of A_Y and A_X. The slope of regression represents the relation between extinction at the two spectral bands. These values are used to derive the average extinction curves for the areas occupied by dust.

4. Results and discussion

4.1. Extinction curve

The calculated values of the slope of the regression lines alongwith the values reported by Savage & Mathis (1979) for our Galaxy are given in Table 2. The value of R_V, i.e. the ratio of total extinction A_V in the V band to the selective extinction E_{B-V} between B and V bands, is found to be 2.70$\pm$0.28, whereas its Galactic value is reported as 3.1 (Savage & Mathis 1979, Rieke & Lebofsky 1985). The smaller value of R_V as compared to that of our Galaxy shows that the average dust particle size of this galaxy is smaller than in our Galaxy. Goudfrooij et al. (1994b) have shown that the dust particles appear larger because of foreground light and/or forward scattering, implying that the dust particle size in this galaxy is indeed smaller than in our Galaxy. The extinction curve for this galaxy is plotted alongwith the Galactic extinction curve in Fig. 3. The extiction curve of NGC 2076 runs almost parallel to the Galactic extinction curve which shows that the properties of dust in it are similar to those in our Galaxy.

Table 2. Linear fits of extinction

X	Y	Best Slope	Corr. Coeff.	S.M. Slope
A_V	A_B	1.09$\pm$0.01	0.98	1.32
A_V	A_R	0.71$\pm$0.02	0.97	0.75
A_V	A_I	0.55$\pm$0.01	0.85	0.48
E(B-V)	A_B	3.70$\pm$0.33	0.70	4.10
E(B-V)	A_V	2.70$\pm$0.28	0.60	3.10
E(B-V)	A_R	1.83$\pm$0.23	0.58	2.32
E(B-V)	A_I	1.32$\pm$0.19	0.63	1.50

Using the extinction curve and extinction efficiency Q_{ext} of spherical dielectric grains (Greenberg 1968), we have tried to estimate the relative dust grain size responsible for extinction. From Fig. 3, it is obvious that the extinction curve varis linearly with the inverse wavelength in the optical part of the spectrum, which is also consistent with the prediction that for small grain size $x < 1$, $Q_{ext} \propto \lambda^{-1}$, where $x = \frac{2*\pi*a}{\lambda}$ is the grain size in dimensionless parameters and 'a' is the grain radius. The shift of extinction curve along the increasing value of λ^{-1} for a fixed value of Q_{ext} essentially indicates the decrease in characteristic particle size 'a'. The relative grain size ($< a >/a_{Gal}$; a_{Gal} is the

characteristic grain size of dust in our Galaxy) is obtained by shifting the extinction curve along $1/\lambda$ axis untill it best matches with the Galactic curve. The relative grain size thus obtained is $< a >/a_{Gal}$ =0.89 $\pm$ 0.07.

4.2. Dust mass estimation

– Dust mass from total extinction:
We have made an attempt to derive the dust content of this galaxy using the extinction values, obtained in section 3.1. For a given grain size distribution n(a), the specific grain mass density ρ_d, and length of the dust column l_d, the dust column density can be calculated using the relation

$$\Sigma_d = \int \frac{4}{3}\pi a^3 \rho_d n(a) da \times l_d \quad (3)$$

We have used the dust size distribution of Mathis et al. (1977) i.e.

$$n(a) = n_0 a^{-3.5} \quad (a_- \leq a \leq a_+) \quad (4)$$

The upper and lower dust particle sizes are taken to be

$$a_+ =< a > /a_{Gal} \times 0.22\mu m \quad \text{and} \quad a_- = 0.005\mu m, \quad (5)$$

respectively. The value of $< a > /a_{Gal}$ is 0.89$\pm$0.07 for NGC 2076 as calculated in section 4.1. We have assumed that the dust is composed of silicate and graphite grains with equal abundance ratio and typical grain size of $a_{silicate}$ = 0.1μm, $a_{graphite}$ = 0.05μm. Extinction efficiencies are taken from literature and parametrized for the V-band extinction (Goudfrooij et al. 1994b). The dust mass estimated in this manner turns out to be $3.2\times10^6 M_\odot$.
We have also estimated the neutral hydrogen mass and dust mass from the optical color-excess using the relation given by Bohlin et al.(1978) and assuming that gas-to-dust ratio of 100 is valid for NGC 2076 also. It gives mass of total neutral hydrogen as 1.8 $\times$ 10^8 $M_\odot$ and dust mass as 1.8 $\times$ 10^6 $M_\odot$. The dust mass calculated using optical color-excess involves the assumption of gas-to-dust ratio similar to the Galactic value, which may not be a good approximation for early-type galaxies.
– Dust mass from FIR data:
We have made use of FIR flux from Knapp et al. (1989) to derive dust temperature, dust mass, total FIR luminosity and mass of the molecular hydrogen. Dust mass has been estimated from the relation in Thronson et al. (1986). The derived temperature of dust is 36 K, Infra-red luminosity is 2.98 $\times 10^{11}$ $L_\odot$, dust mass is 3.67 $\times$ 10^6 $M_\odot$.

In absence of neutral as well as molecular hydrogen observations it is very difficult to have a reliable estimate of total ISM content of this galaxy. However, estimation of dust content from FIR as well as optical data does indicate that it contains significant amount of ISM. A rough estimate of molecular hydrogen mass may be obtained from the dust mass derived from FIR data and making some assumptions about the ratio of molecular hydrogen to dust mass. Taking a value of $\sim$ 700 for this ratio as given by Wiklind et al. (1995) for early-type galaxies, the molecular hydrogen mass turns out to be $\sim 4.6 \times 10^9$ $M_\odot$. Thus, this galaxy appears to be extremely ISM rich.

4.3. Star formation rate (SFR) and efficiency

The dust temperature of 36 K is similar to the findings of Brosch et al. (1991), which shows that this galaxy contains warm dust (Sanders & Mirabel 1996). By virtue of its log(f(60 μm)/f(100μm)) = - 0.33 and log(f(12μm)/f(25μm)) = - 0.07 ratio it occupies an intermediate position in the phenomenological diagram of Helou (1986), where the cool component as well as the newly formed massive stars are responsible for heating the dust, and more than 50% of the IR emission can be attributed to young stars. This indicates an ongoing star formation in this galaxy. Therefore, we have tried to estimate the SFR using the FIR luminosity and total blue luminosity of NGC 2076.

The present day star formation rate, averaged over past 2×10^6 yrs. under the assumption that all the FIR emission comes from dust heated by young stars is estimated using the relation
$\dot{M}_{IR}(all)$ = 6.5$\times$ 10^{-10} $L_{FIR}(L_\odot)$
given by Thronson & Telesco (1986). It gives SFR of 110.5$M_\odot yr^{-1}$. However, considering the phenomenological model of Helou (1986) the expected SFR will be $\sim$ 55 - 60 $M_\odot yr^{-1}$.

The SFR for massive O, B, A stars, obtained from the relation
$\dot{M}_{OBA}$ = 7.7 $\times$ 10^{-11} $L_{tot}(L_\odot)$,
given by Young et al. (1986), and assuming that the star formation process lasts for $\sim$ 10^9 yrs., is 13.63 $M_\odot$ yr^{-1}. This estimate would be true provided that the observed luminosity is produced primarily by massive O, B, A type stars and therefore it can be taken as an upper limit of SFR for NGC 2076.

Gallagher et al. (1984) have used the total blue luminosity of a galaxy to estimate the recent SFR averaged over the past (0.4 - 6)10^9 yrs.:
$\dot{M}_\odot$ yr^{-1} = 6.5 $\times 10^{-9}$ $L_B(L_\odot)$.
Applying this relation for the case of NGC 2076 gives a value of 20.9 $M_\odot$ yr^{-1} for the recent SFR averaged over the life time of stars, that dominate the blue light.
The comparison of SFR calculated for different scenarios reveals that the present day SFR averaged over 2×10^6 yrs. is much higher than the SFR for massive O, B, A stars averaged over $\sim$ 10^9 yrs.. The SFR for low as well as high mass stars averaged over (0.4 - 6)10^9 yrs. is 20.9$M_\odot$ yr^{-1}, which is greater than but consistent with its value for massive O, B, A type stars. This indicates that the star formation rate for this galaxy is rather high in the present epoch.

4.4. Origin of dust

A consensus is growing for an external origin of dust in early-type galaxies. The prominent dust lane observed in NGC 2076 may be attributed to either merger or interaction with a gas-rich companion. We do not find any suitable companion galaxy from which this galaxy could have accreted the observed dust. How-

ever, the observed strong dust obscuration and FIR emission in this galaxy suggest that it may have accreted an entire gas-rich galaxy. Further, very high star formation rate at the present epoch indicates that the cannibal process might have occured in not-so-distant past. Detailed invesigations, specially on its kinematics, are needed to arrive at any firm conclusion as regards the origin of dust in NGC 2076.

5. Conclusions

The main conclusions of present work are as follows:

1. Extinction curve for NGC 2076 is similar to that in our Galaxy. The extinction varies linearly with inverse wavelength with a ratio of total to selective extinction $R_V = 2.70 \pm 0.28$, which indicates that the dust grain size in this galaxy is smaller than the Galactic dust particle size.

2. Dust mass from total extinction is estimated to be $3.2 \times 10^6 M_\odot$.

3. Far infrared flux imply a dust temperature of $\sim$ 36 K, and dust mass 3.67×10^6 $M_\odot$. The comparison of star formation rates calculated for different scenarios reveals that this galaxy is undergoing an intense burst of star formation in the present epoch.

Acknowledgements. One of us (SKP) is Senior Associate of IUCAA and he expresses his sincere thanks to Professor J. V. Narlikar, Director, IUCAA for providing support and facilities which made this study possible. We are thankful to the time allocation committee, VBO, Kavalur for providing us observing time and the observatory staff for their generous support during observations. We express our sincere thanks to Dr. N. Brosch who referred the paper and offered his critical comments. This research has made use of the NASA/IPAC Extragalactic Database (NED) which is operated by the Jet Propulsion Laboratory, California Institute of Technology under contract with the National Aeronautics and Space Administration.

References

Barlow M. 1978, MNRAS 183, 367.
Bertola F., Galleta G., 1978, ApJ Letts. 226, L115.
Boisson C., Durrel F., Balkowski C., Proust D., 1994, A&ASS 100,583.
Bohlin R.C., Savage B.D., Drake J.R., 1978, ApJ 224, 132.
Brosch N., Greenberg J.M., Grosbol P., 1985, A&A 143, 399.
Brosch N., Almoznino E., Grosbol P., Greenberg J.M., 1990, A&A 233, 341.
Brosch N., Loinger F., 1991, A&A 249, 327.
Caldwell N., 1984, ApJ 278, 96.
Condon J.J., Helou G., Sanders D.B., Soifer B.T., 1996, ApJSS 103, 81.
de Jong T., Norgaard-Nielsen H.U., Hansen L., Jorgensen H.E., 1990, A&A 232, 317.
de Vaucouleurs G., de Vaucouleurs A., Corwin H.G., Buta R.J., Paturel G., Fouque P., 1991 *Third Reference Catalogue of Bright Galaxies*, Springer, New York (RC3).
Draine B.T., Saltpeter E., 1979, ApJ 231, 77.
Ebneter K., Djorgovski S., Davis M., 1988, AJ 95, 422.
Ebneter K., Balick B., 1985, AJ 90, 183.
Fabbiano G., Kim D.W., Trinchieri G., 1992, ApJSS 80, 531.
Fabian A.C., Thomas P.A., 1987 in *Structure and Dynamics of Elliptical Galaxies, IAU Symposium No. 127*, ed. P.T. de Zeeuw, Dordrecht: Reidel, p. 155.
Faber S.M., Gallagher J.S., 1976, ApJ 204, 365.
Forman W., Jones C., Tucker W., 1985, ApJ 293, 102.
Gallagher J.S., Hunter D.A., Tutukov A.V., 1984, ApJ 284, 544.
Goudfrooij P., Hansen L., Jorgensen H.E., Norgaard-Nielsen H.U., 1994a, A&ASS 105, 341.
Goudfrooij P., de Jong T., Hansen L., Norgaard-Nielsen H.U., 1994b, MNRAS 271, 833.
Greenberg J.M., 1968, in *Nebulae and Interstellar matter, Stars and Stellar systems Vol. VII*, eds. B.M. Middlehurst & L.H. Aller, Chicago: University of Chicago Press, p.221.
Gunn J.E., 1979, in *Active Galatic Nuclei*, ed. Hazard C. and Mitton S., Cambridge Univ. Press, p. 213.
Habe A., Ikeuchi S., 1985, ApJ 289, 540.
Habe A., Ikeuchi S., 1988, ApJ 326, 84.
Hawarden T.G., Elson R.A.W., Longmore A.J., Tritton S.B., Corwin H.G., 1981, MNRAS 196, 747.
Helou G., 1986, ApJ 311, L33.
Jaffe W., Ford H.C., O'Connell R.W., van den Bosch F.C., Ferrarese L., 1994, AJ 108, 1567.
Jedrzejewski R.I., 1987, MNRAS 226, 747.
Jura M., Kim D.W., Knapp G.R., Guhathakurta P., 1987, ApJ 312, L11.
Kim D.W., 1989, ApJ 346, 653.
Knapen J.H., Hes R., Beckman J.E., Peltier R.F., 1991, A&A 241, 42.
Knapp G.R., Guhathakurta P., Kim D.W., Jura M., 1989, ApJS 70, 329.
Knapp G.R., Turner E.L., Cunniffe P.E., 1985, AJ 90, 454.
Lees J.F., Knapp G.R, Rupen M.P., 1991, ApJ 379, 177.
Lequeux J., 1988, in *Dust in the Universe*, eds. Bailey M.E., Williams D.A., Cambridge University Press, Cambridge.
Mathis J.S., Rumpl W., Nordsieck K.H., 1977, ApJ 217, 45.
Mollenhoff C., Hummel E., Bender R., 1992, A&A 255, 36.
Phillips M.M., Jenkins C.R., Dopita, M.A., 1986, AJ 91, 1062.
Rieke G.H., Lebofsky M.J., 1985, ApJ 288, 618.
Rodgers A.W., 1978, ApJ 219, L7.
Rowan-Robinson M., 1992, MNRAS 258, 787.
Sadler E.M. 1984, AJ 89, 53.
Sarazin C.L., 1986, Rev. Mod. Phys. 58, 1.
Savage B.D., Mathis J.S., 1979, ARA&A 17, 73.
Schweizer F. 1987, in *Structure and Dynamics of Elliptical Galaxies*, *IAU Symposium No. 127*, ed. P.T. de Zeeuw, Dordrecht: Reidel, p.109.
Thronson H., Telesco C., 1986, ApJ 311, 98.
van Albada T.S., Kotanyi C.G., Schwarzschild M., 1982, MNRAS 198, 303.
Walterbos R.A.M., Kennicutt R.C., 1988, A&A 198, 61.
Wang Z., Kenny J.P.D., Ishizuki S., 1992, AJ 104, 2097.
Wiklind T., Combes F., Henkel, C., 1995, A&A 297, 643.
Young J.S., Schloerb F.P., Kenney J.D., Lord S.D., 1986, ApJ 304, 443.